Hydrol. Earth Syst. Sci. Discuss., 8, 9395–9434, 2011
www.hydrol-earth-syst-sci-discuss.net/8/9395/2011/
doi:10.5194/hessd-8-9395-2011

Hydrology and Earth System Sciences Discussions

The past and future changes of streamflow in Poyang Lake Basin, Southeastern China

S. L. Sun[1,2], H. S. Chen[1], W. M. Ju[3], J. Song[4], J. J. Li[5], Y. J. Ren[6], and J. Sun[6]

[1]Key Laboratory of Meteorological Disaster of Ministry of Education, Nanjing University of Information Science & Technology, Nanjing, China
[2]Applied Hydrometeorological Research Institute, Nanjing University of Information Science & Technology, Nanjing, China
[3]International Institute for Earth System Science, Nanjing University, Nanjing, China
[4]Department of Geography, Northern Illinois University, Chicago, USA
[5]The Agrometeorological Center of Sichuan Province, Chengdu, China
[6]Wuhan Regional Climate Center, Wuhan, China

Received: 14 September 2011 – Accepted: 6 October 2011 – Published: 24 October 2011

Correspondence to: S. L. Sun (ppsunsanlei@163.com)

Published by Copernicus Publications on behalf of the European Geosciences Union.

Abstract

Water resources have a close relationship with climate. The changes of streamflow affect the exploitation and utilization of water resources directly, and the social security and the stability of ecological system. Meteorological observations at 79 weather stations, and datasets of streamflow and river level at 4 hydrological stations were collected to analyze the changes of streamflow and underlying drivers in four typical watersheds within Poyang Lake Basin during the period from 1961 to 2000. The contributions of different factors to the changes of streamflow in four typical watersheds were quantitatively quantified using water balance equation. Then, the possible future change of streamflow was assessed using precipitation and evaporation projected by different GCMs under three different emission scenarios, including medium greenhouse gases emission scenario (SRESA1B), high greenhouse gases emission scenario (SRESA2), and low greenhouse gases emission scenario (SRESB1).

The change of streamflow exhibited different characteristics the four watersheds exist different increasing trends during 1961 to 2000. The increase in streamflow in Meigang and Gaosha watersheds was at the 5 % significance level, with increasing rate of 4.80 $m^3 s^{-1} yr^{-1}$ and 1.29 $m^3 s^{-1} yr^{-1}$, respectively. The increase in precipitation is the biggest contributor to streamflow increment in Meigang Gaosha, and Xiashan watersheds, while the decrease in evaporation is the major explainer for streamflow increment in Saitang watershed. Radiation and wind have larger contributions than actual vapor pressure and mean temperature to evaporation and streamflow.

If soil water storage will not change in the future, with the increasing precipitation and the decreasing evaporation (not including the SRESB1 in Xiashan watershed), the streamflow shows an uptrend. Furthermore, the largest increase of Meigang watershed (+4.13 %) and Xiashan watershed (+3.84 %) appear under SRESA1B scenario while the increase of Saitang watershed (+6.87 %) and Gaosha watershed (+5.15 %) in SRESB1 scenario.

HESSD

8, 9395–9434, 2011

1 Introduction

Changes in water resources are affected by many aspects of environment, economy and society and have the potential to severely affect environmental quality, economic development and social well-being (Kundzewicz et al., 2007; Zhang et al., 2007). Components of the water cycle are influenced by variations of precipitation, evaporation, temperature, and so on and natural variability of water resources is associated closely with climate change (Nash et al., 1991; Liu et al., 1993; Milly et al., 2005; Gedney et al., 2006; Oki et al., 1995). As an important part of the water cycle (Oki and Kanae, 2006), streamflow changes can significantly affect water resources, society safety and ecosystem health. It can also be used as an indicator of climate change owing to the intimate linkage of water cycling with climate.

The Intergovernmental Panel on Climate Change (IPCC, 2007) pointed out that the average global temperature had increased by $0.74 \pm 0.18^{\circ}$ in the past 100 yr, which impacted on the natural ecosystems and environment significantly. The global warming may even be speeded up in the future, consequently leading to an increase in both floods and droughts. Therefore, changes in water resources and underlying driving foreces for such changes have become hot issues all over the world (Andréasson et al., 2004; Christensen and Lettenmaier, 2007; Frederick et al., 1997; Gül et al., 2010; Lins et al., 1999; Liu et al., 2009; Null et al., 2010; Piao et al., 2007; Thodsen et al., 2007; Vörösmarty et al., 2000; Xu et al., 2010; Zhang et al., 2001). Andréasson et al. (2004) discussed the impacts of the climate change on streamflowunder three anthropogenic CO_2 emission scenarios with a hydrology model (HBV) and concluded that the influences of climate change on hydrology cycle varied geographically. Lins et al. (1999) applied the nonparametric Mann-Kendall test method to study temporal trends of streamflow at 395 gauging stations across the USA and suggested that streamflow showed increasing trends in most regions, except for the northwest and the southeast Pacific. Zhang et al. (2001) pointed out that streamflow decreased significantly from 1947 to 1996 in the southern of Canada, and it also decreased in most

HESSD
8, 9395–9434, 2011

months, especially in August and September. Xu and Liu et al. (2010) analyzed the trends of major hydroclimatic variables from 1960 to 2007 in the Tarim River basin of China and concluded that the impacts of increasing air temperature on streamflow showed different characteristics, depending on location and seasons. Increasing temperature caused runoff to increase in mountainous regions due to enhanced snowmelt and glacier-melt in spring and to decreases in plain areas due to the increasing actual evaporation in summer.

Along with global warming, the average temperature in China has experienced a dramatic increase over the last century (Ding et al., 1994; Zhai et al., 2004; Zhang et al., 2005; Yang et al., 2010; Li et al., 2010), leading to critical water stress [The Standing Committee of the National People's Congress (NPC) of the People's Republic of China 1994]. The Yangtze River Basin is one of the most advanced economic regions and the most serious flooding regions in China. Over the past years, as temperature and precipitation increasing, the occurrence frequencies and intensity of floods in this basin have increased obviously and significantly (Hu et al., 2007), resulting in serious economic losses. The projected increase of 2.7° in temperature in the 21st century will induce precipitation and streamflow to increase by 10 % (Gao et al., 2001) and 37 % (IPCC, 2001) respectively, and the extreme events of rainfall may take place frequently. Moreover, the probabilities of the most serious floods occurring in periods of 10-, 100-, 1000-yr, and even longer (such as floods in 1870, 1954 and 1998) increase. As the largest freshwater lake basin in China, Poyang Lake exchanges water with the Yangtze River and acts as the reservoir of floods in the middle and lower reaches of the Yangtze River. Its capacity of flood diversion has decreased continuously with the ecological and environmental damages (the serious soil and water losses, and the reduction of lake areas and volume). The surface area of this lake shrunk by 25 % and its capacity decreased by 22 % from 1954 to 1998 (Jiang, 2007), resulting in more vulnerability of the basin to flood. Both droughts and floods have occurred frequently and alternatively here in recent decades. Moreover, floods have increased in severity since 1990. In the summers of 1998, 1996, and 1995, this basin experienced three most severe floods (in

HESSD
8, 9395–9434, 2011

descending order) in the last 50 yr (Wang et al., 2000; Jiang and Shi, 2003; Shankman et al., 2006).

Recently, the responses of hydrological cycle in Yangtze River Basin to climate change have received more and more attention. The trend test and change-point analysis have been carried out using the annual maximum, annual minimum and annual mean discharge rates reordered at the Yichang gauging station during the period from 1882 to 2001 by Xiong et al. (2004). They reported that, at the 5 % significance level, the annual maximum discharge rate did not have any statistically significant trend, but the annual minimum and the annual mean discharge rates significantly decreased by 8 % and 6 %, respectively. Using the SWAT (Soil and Water Assessment Tools) model, Guo et al. (2008) studied annual and seasonal responses of streamflow to climate and land-use changes in the Poyang Lake basin, China, and revealed that climate had a dominant effect on annual streamflow. Land-use changes might have a moderate impact on annual streamflow while it strongly influenced seasonal variations of streamflow and altered the annual hydrograph of this basin. Chen et al. (2007) found that mean annual, spring and winter runoff decreased at 5 % significance levels in the Hanjinag Basin, caused by the integrated effects of precipitation and temperature. They also projected increasing trends of runoff during the period from 2021 to 2050 under 3 different climate initial fields using a two-parameter water balance model. Zhao et al. (2009) declared that streamflow were more sensitive to variations in precipitation than to variations of potential evaporation in Poyang Lake Basin.

Previous studies mainly focused on the effects of long-term variability of precipitation and temperature on water resources. The influences of other climatic variables, such as radiation, wind speed, and vapor pressure, on water cycle have not been thoroughly studied. In this paper, the roles of various climatic variables in streamflow of Poyang Lake Basin, southeastern China were quantified using historical streamflow and climate data on the basis of water balance. The future trends of streamflow in this basin under three different climate change scenarios were further projected.

HESSD
8, 9395–9434, 2011

2 Study area, data used and methods

2.1 Study area

Poyang Lake Basin is located in the middle reaches and the south bank of Yangtze River, China, covering totally an area of 1.6×10^5 km^2, accounting for 9 % of Yangtze River Basin and nearly 96.85 % of the land mass of Jiangxi Province (Fig. 1). The size of the lake water body fluctuates greatly in season. The water body area can exceed a maximum area of 4000 km^2 in summer and shrinks to less than 3000 km^2 in fall and winter. This lake receives water primarily from Ganjiang River, Xiushui River, Fuhe River, Raohe River, and Xinjiang River. The topography in Poyang Lake Basin is diverse, including mountains, hills, and alluvial plains. Mountains spread mainly in the western and eastern parts, with a maximum elevation of 1800 m above the sea level (m.a.s.l), while low alluvial plains are primarily in its central areas, mainly distributed in areas along Ganjiang River.

Four typical watersheds inside Poyang Lake Basin were selected for studying the historical trends of streamflow. They are Meigang, Xiashan, Saitang, and Gaosha watersheds, located in the northeast, southeast, middle-west, and northwest parts of Poyang Lake Bain (Fig. 1), respectively. The boundaries of watersheds were delineated using the hydrological analysis tools of ArcGIS 9.2 software package based on the 90 m STRM_Version1 (from internet site: http://dds.cr.usgs.gov/srtm/) Digital Elevation Model (DEM) data. The drainage areas are 1.53×10^4 km^2, 3.07×10^3 km^2, 5.22×10^3 km^2 and 1.59×10^4 km^2 for Meigang, Xiashan, Saitang, and Gaosha, respectively.

The study area belongs to the subtropical monsoon climate zone with a temperate and humid climate. Sunlight is abundant here. Temperature and precipitation both exhibit distinct seasonality (Fig. 2). In all watersheds, monthly mean temperature (the left panel of Fig. 2a) increases from January to July and then decreases. The annual mean temperature during 1961 ~ 2000 was 16.6° in the Saitang watershed, while it is above 17.9° in other three watersheds. Monthly total precipitation (the left panel

HESSD
8, 9395–9434, 2011

of Fig. 2b) increases very quickly from January to June and then decreases sharply. The annual precipitation during 1961 ~ 2000 is about 1640 mm in Meigang and Saitang watersheds and about 1690 mm in Gaosha and Xiashan watersheds.

2.2 Data

2.2.1 Meteorological and hydrological data

The daily meteorological data during 1961 to 2000 from 79 weather stations (73 and 6 stations inside and outside Poyang Lake Basin) are used in this study (Fig. 1), including daily precipitation (mm), 20 cm caliber pan evaporation (mm), sunshine percentage (%), wind speed ($m\,s^{-1}$), maximum temperature (°), minimum temperature (°) , mean temperature (°) , actual water vapor pressure (kPa), and relative humidity of air (%). As there are only 2 weather stations with radiation observed in the study area, the methods proposed by Wang (2006) and Tong (1989) are used to calculate daily total incoming solar radiation (MJ $m^{-2}\,day^{-1}$) and long-wave radiation (MJ $m^{-2}\,day^{-1}$), respectively. Net radiation (MJ $m^{-2}\,day^{-1}$) is calculated as the summation of net solar radiation and long-wave radiation. The Spline Function Method in the ArcGIS 9.2 platform is employed to interpolate annual mean/total values of climate variables of 79 stations into a resolution of 1 × 1 km. The time series of regional averages of climate variables for each watershed were calculated for the period from 1961 to 2000 to assess the impacts of climate on streamflow.

Hydrological data used this study include daily streamflow ($m^3\,s^{-1}$) and river level (m) measured at Meigang, Saitang, Gaosha, and Xiashan gauge stations (Fig. 1).

2.2.2 The future climate scenarios

The contemporary climate and future climates projected by different general circulation models (GCMs) were used in this study (Table 1). The contemporary climate was projected with the contemporary climate scenario of 20C3M. Future climates

HESSD
8, 9395–9434, 2011

were projected under three different scenarios of greenhouse gasses emission, including medium greenhouse gases emission scenario (SRESA1B), high greenhouse gases emission scenario (SRESA2), and low greenhouse gases emission scenario (SRESB1). The datasets from GCMs used were monthly precipitation and latent heat flux which was converted into monthly evaporation. The details about GCMs used can be found on http://www-pcmdi.llnl.gov/ipcc/model_documentation/ipcc_model_documentation.php.

2.2.3 Other data

The land use/land cover dataset in 1995 was downloaded from Environmental & Ecological Science Data Center for West China, National Natural Science Foundation of China (http://westdc.westgis.ac.cn). The SPOT VGT-NDVI datasets in 1999 and 2000 were downloaded from the VITO archive (http://www.vgt.vito.be). The spatial resolutions of these two datasets are 1 × 1 km.

2.3 Methods

2.3.1 Detecting the temporal trends of climate and hydrology

Trends of a climate/hydrology variable can be fitted using the following linear equation:

$$\hat{x}_t = a_0 + a_1 t \ (t = 1, 2, \ldots, n.) \quad (1)$$

where $\hat{x}_t$, a_0, a_1, and t represent the fitted value of a variable, the intercept, the temporal variability, and time, respectively; n ($n = 40$) is the sample number of a variable. A positive value of a_1 indicates an increasing trend, vice versa. A larger magnitude of a_1 denotes a stronger increasing or decreasing trend.

HESSD
8, 9395–9434, 2011

2.3.2 Water balance for a watershed

The study area has a subtropical climate. Snowfall is sparse. Therefore, for a watershed, water balance is calculated as:

$$R = a \times P - E + W + q \quad (2)$$

where R is the streamflow (the sum of surface and underground runoff) measured at the outlet of a watershed; a is the ratio of throughfall to total precipitation above canopy; P is precipitation amount; E is the actual evaporation; W is the change of water storage in the watershed; q is the water consumption from the watershed.

In reality, q is small in a closed watershed. For similarity, q is assumed to be zero here. E is calculated from 20 cm caliber pan evaporation measurements:

$$E = b \times E_{\text{pan}} \quad (3)$$

where b is the coefficient converting pan evaporation to actual evaporation; E_{pan} is the evaporation measured with the 20 cm caliber pans.

Some rainfall is intercepted by vegetation canopy (Crockford et al., 2000; Hölscher et al., 2004; Huang et al., 2005). The intercepted rainfall is not involved in the process of runoff yield. Only the throughfall affects streamflow. The parameter a in Eq. (2) depends on canopy density and rainfall intensity.

In the study area, precipitation shows considerable interannual variability due to the monsoon climate. The interannual variations of water storage can not be ignored in the calculation of water balance for a watershed using Eq. (2). However, there is no any observation of water storage available at the watershed level. As an approximation, we use the intra-annual variability of river level (ΔWL) as a surrogate of W. ΔWL is defined as the difference between the mean water level of the last 10-day in December and that of the first 10-day in January in the same year. W is calculated as:

$$W = c \times \Delta\text{WL} \quad (4)$$

HESSD
8, 9395–9434, 2011

When the studied time period (n) is long enough, W satisfies the following equation:

$$\frac{1}{n}\sum_{1}^{n} W_i = \frac{1}{n}\sum_{1}^{n}(c \times \Delta \mathrm{WL}_i) \approx 0 \quad (5)$$

After units conversion, Eq. (1) can be rewritten as:

$$R = (a \times P/1000 - b \times E_{\mathrm{pan}}/1000 + c \times \Delta \mathrm{WL}) \times A/(\mathrm{yd} \times 24 \times 3600) \quad (6)$$

where A (m^2) is the watershed area; yd (day) is the Julian day in a year; a, b and c are parameters to be optimized using observed hydrological and climate data.

2.3.3 Partition of the influences of different climatic variables on streamflow

Evaporation is a key component of water balance in a watershed. Temperature, radiation, wind speed, actual vapor pressure are the major climatic factors to influence actual evaporation. In term of the Penman equation, evaporation from a pan (Sun et al., 2010) can be expressed as:

$$E_{\mathrm{pan}} = \frac{ET_{\mathrm{R}} + ET_{\mathrm{A}}}{K_{\mathrm{p}}}\ ET_{\mathrm{R}} = \frac{\Delta}{\Delta+\gamma}\frac{R_{\mathrm{n}} - G}{\lambda}, ET_{\mathrm{A}} = \frac{\gamma}{\Delta+\gamma} f(U_2)(e_{\mathrm{s}} - e_{\mathrm{a}}) \quad (7)$$

where ET_{R} (mm day^{-1}) and ET_{A} (mm day^{-1}) are the reference evaporation related to the radiation and aerodynamic terms, respectively; K_{p} (dimensionless) is the pan coefficient and set as 0.67 (Xu et al., 2006); Δ(kPa $^{\circ}\mathrm{C}^{-1}$) is the slope of the saturation vapor pressure curve; λ (kPa $^{\circ}\mathrm{C}^{-1}$) is the psychometric constant. R_{n} (MJ $\mathrm{m}^{-2}\,\mathrm{day}^{-1}$) is the net radiation; G (MJ $\mathrm{m}^{-2}\,\mathrm{day}^{-1}$) is the soil heat flux density and assumed to be zero at the annual time step; $f(U_2)$ (mm $\mathrm{kPa}^{-1}\,\mathrm{day}^{-1}$) is the function of wind speed (Sun et al., 2010); U_2 is the wind speed at 2 m height and converted from the wind speed at 10 m height (U_{10}); e_{s} (kPa) the saturation vapor pressure; e_{a} (kPa) is the vapor pressure. The various items in Eq. (7) are calculated following Allen et al. (1998).

HESSD
8, 9395–9434, 2011

The influences of different factors on streamflow rate are quantified through differentiating Eqs. (6) and (7), i.e.

$$\frac{\mathrm{d}R_{\mathrm{yr}}}{\mathrm{d}t} = \left[\frac{\mathrm{d}(\frac{a}{1000}\times P_{\mathrm{yr}})}{\mathrm{d}t} - \frac{\mathrm{d}(\frac{b}{1000}\times E_{\mathrm{pan,yr}})}{\mathrm{d}t} + \frac{\mathrm{d}(c\times \Delta \mathrm{WL}_{\mathrm{yr}})}{\mathrm{d}t}\right]\times\frac{A}{\mathrm{yd}\times 24\times 3600}$$

$$= \left\{\frac{\mathrm{d}(\frac{a}{1000}\times P_{\mathrm{yr}})}{\mathrm{d}t} - \frac{\mathrm{d}[\frac{b}{1000}\times(\frac{ET_{\mathrm{R}}+ET_{\mathrm{A}}}{K_{\mathrm{P}}})]}{\mathrm{d}t} + \frac{\mathrm{d}[c\times\Delta \mathrm{WL}_{\mathrm{yr}}]}{\mathrm{d}t}\right\}\times\frac{A}{\mathrm{yd}\times 24\times 3600}$$

$$= \underbrace{\frac{a}{1000}\frac{\mathrm{d}P_{\mathrm{yr}}}{\mathrm{d}t}\frac{A}{\mathrm{yd}\times 24\times 3600}}_{P^*} + \underbrace{\left(-\frac{b}{1000K_{\mathrm{p}}}\frac{\partial ET_{\mathrm{R,yr}}}{\partial R_{\mathrm{n}}}\frac{\mathrm{d}R_{\mathrm{n}}}{\mathrm{d}t}\frac{A}{\mathrm{yd}\times 24\times 3600}\right)}_{R_n^*}$$

$$+ \underbrace{\left\{-\frac{b}{1000K_{\mathrm{p}}}\frac{\partial ET_{\mathrm{A,yr}}}{\partial\left[f(U_2)_{\mathrm{yr}}\right]}\frac{\mathrm{d}\left[f(U_2)_{\mathrm{yr}}\right]}{\mathrm{d}U_{2,\mathrm{yr}}}\frac{\mathrm{d}U_{2,\mathrm{yr}}}{\mathrm{d}t}\frac{A}{\mathrm{yd}\times 24\times 3600}\right\}}_{U^*}$$

$$+ \underbrace{\frac{b}{1000K_{\mathrm{p}}}\frac{\partial ET_{\mathrm{A,yr}}}{\partial e_{\mathrm{a,yr}}}\frac{\mathrm{d}e_{\mathrm{a,yr}}}{\mathrm{d}t}\frac{A}{\mathrm{yd}\times 24\times 3600}}_{e_a^*}$$

$$+ \underbrace{\left\{-\frac{b}{1000K_{\mathrm{p}}}\left[\left(\frac{\partial ET_{\mathrm{R,yr}}}{\partial\Delta}+\frac{\partial ET_{\mathrm{A,yr}}}{\partial\Delta}\right)\frac{\mathrm{d}\Delta}{\mathrm{d}T_{\mathrm{ave,yr}}}+\frac{\partial ET_{\mathrm{A,yr}}}{\partial e_{\mathrm{S,yr}}}\frac{\mathrm{d}e_{\mathrm{S,yr}}}{\mathrm{d}T_{\mathrm{ave,yr}}}\right]\frac{\mathrm{d}T_{\mathrm{ave,yr}}}{\mathrm{d}t}\frac{A}{\mathrm{yd}\times 24\times 3600}\right\}}_{T_{\mathrm{ave}}^*}$$

$$+ \underbrace{c\frac{d(\Delta WL_{\mathrm{yr}})}{\mathrm{d}t}\frac{A}{\mathrm{yd}\times 24\times 3600}}_{W^*}$$

HESSD
8, 9395–9434, 2011

$$= \underbrace{P^* + R_n^* + U^* + e_a^* + T_{ave}^*}_{E^*} + W^* \quad (8)$$

where P_{yr} and $E_{pan,yr}$ is annual total precipitaion and pan evaporation. P^*, E^*(R_n^*, U^*, e_a^* and T_{ave}^*), and W^* represent to the effects of change in annual precipitation, evaporation (related to net radiation, wind speed, actual vapor pressure and mean temperature) and intra-annual variability of river level on sftreamflow, respectively.

2.3.4 Changes of precipitation and evaporation projected by GCMs and their contributions to streamflow

Precipitation and evaporation projected by GCMs were extracted for the area of 110° E and 120° E, and 20° N and 35° N. Then, the projected precipitation and evaporation (20C3M) were interpolated with the Spline Function method in the ArcGIS 9.2 platform. The area means of projected precipitation and evaporation during 2061 to 2100 were calculated for different watersheds. In order to constrain the effects of model biases on assessing the future changes of streamflow caused by climate change, precipitation and evaporation during 2061 to 2100 were calculate as:

$$\Delta \mathrm{var}^k = \frac{1}{n} \sum_i^n \left(\frac{\mathrm{var}^{obs}}{\mathrm{var}_i^{20C3M}} \times \mathrm{var}_i^k - \mathrm{var}^{obs} \right) \quad (9)$$

where var denotes the mean of precipitation/evaporation; $\Delta \mathrm{var}^k$ represents the change of the mean of precipitation/evaporation during 2061 to 2100 projected by GCMs relative to the mean of precipitation/evaporation observed during 1961 to 2000; k denotes the number of future climate scenarios; n is the number of GCMs projecting precipitation/evaporation for scenario k; var_i^k is the mean of precipitation/evaporation during 2061 to 2100 project by the i^{th} GCM for scenario k; var^{obs} represents the mean of precipitation/evaporation observed during 1961 to 2000; var_i^{20C3M} is the mean of precipitation/evaporation projected by the i^{th} GCM for the scenario of 20C3M.

HESSD
8, 9395–9434, 2011

Therefore, the future change of streamflow relative to the observed mean during 1961 to 2000 caused by precipitation or evaporation (ΔR_i) is quantified as:

$$\Delta R_i = \frac{\frac{C}{D} \times \Delta \mathrm{var}^k}{R^{\mathrm{obs}}} \times 100\% \quad (10)$$

Where ΔR_i represents the percent change caused by the single climate variables (precipitation or evaporation); R^{obs} is the mean of observed streamflow during 1961 and 2000; C denotes the coefficient a for precipitation term or b for evaporation term; i denotes precipitation or evaporation; D is 1 and K_p for precipitation and evaporation, respectively.

3 Analysises and results

3.1 Optimized parameters in the water balance equation

Based on the least square method, parameters a, b and c in Eq. (6) were optimized using the observed datasets during the period from1961 to 1990. They differ in different watersheds (Table 2). The validation using the climate and streamflow observations during the period from 1991 to 2000 confirms that the calibrated water balance equation (Eq. 6) is able to capture the interannual variations of streamflow in different watersheds (Fig. 2). The calculated annual mean streamflow is in good agreement with observations in 4 watersheds, with all r (the correlation coefficient between the calculated and the observed streamflow values) values above 0.94 and the signifiance level of 5 %, relative mean error (RME) values in the range from −3.8 to 0.98 %, and root mean squre erroe (RMSE) values ranging from 7.24 to 39.21 $\mathrm{m^3\,s^{-1}}$. Calculated streamflow is slightly larger than the observation in the Meigang watershed, but slightly smaller than observations in other three watersheds. The validation demonstrates that the model developed in this study is applicable to calculate streamflow from climate, pan evaporation and water level data at the watershed scale.

HESSD
8, 9395–9434, 2011

Values of parameters *a*, *b* and *c* in Eq. (6) optimized using the observations during the period from 1961 to 2000 are also listed in Table 2. It shows that the values of these parameters determined using the observations taken in different time periods are very similar, implying the applicability of the parameters values determined using historical data in projecting the future trends of streamflow under different climate scenarios. The parameter values optimized using the datasets measured during the period from 1961 to 2000 were used to investigate the influences of different climatic variables on streamflow.

Parameter *a* is related to the interception capacity of vegetation (e.g. canopy interception and stem interception) and evaporation rate of intercepted water. Wen et al. (1995) quantitatively analyzed the characteristics of rainfall interception of main forest ecosystems in China, and found that interception coefficient (can be expressed as 1-*a*) differed considerably in various forest ecosystems and the mean values usually ranged from 11.4 to 36.5 %. Crockford et al. (2000) and Fan et al. (2007) pointed out that a number of factors could influence canopy interception coefficient, such as rainfall characters (quantity, intensity and duration), wind speed, environment, vegetation types, and vegetation canopy density and so on. The processes of influencing canopy interception were relatively complex. Generally, the interception coefficient of dense canopy is larger than that of canopy with low density. If wind is larger, the interception coefficient will be lower. No great difference exists in monthly rainfall among 4 watersheds (Fig. 2). Figure 4a shows the monthly and annual means of leaf area index (LAI) derived from SPOT VGT-NDVI datasets in years 1999 and 2000. The monthly annual means of 10 m wind speed during the period from 1961 to 2000 for 4 watersheds. For Gaosha and Saitang watersheds, intra-annual variations of rainfall and LAI are asynchrony. Among 4 watersheds, Gaosha watershed has the highest annual mean LAI and lowest wind speed, resulting the smallest value of *a* (0.79) and highest incertpetion coeffcient (1-*a* = 0.21) during the period from 1961 to 2001. Meigang watershed has the highest wind speed and the second lowest LAI (only slightly higher than LAI in Xiashan watershed). Precipitation comes into this watershed mainly in months from

HESSD
8, 9395–9434, 2011

March to June (Fig. 2). During this period, LAI of this watershed is low owing to high percentage (22.60 %) of farmland in this watershed. Two rotations of rice are cultivated here. The early rotation of rice is planted in the middle of April and harvest in late July. During the months from January to June, wind is much stronger here than in other watersheds. The value of parameter *a* is highest among four watersheds. The interception coefficient of this watershed during the period from 1961 to 2000 is only 0.02.

The actual evaporation of a watershed can be calculated using Eq. (2) based on climate and hydrology data. 40-yr mean values of actual evaporation are 585.83 mm, 546.93 mm, 490.91 mm and 607.97 mm in Meigang, Xiashan, Saitang, and Gaosha watersheds, respectively. The differences in actual evaporation can be caused by differences in vegetation types and canopy density, topography, precipitation, wind speed, radiation and atomosphere water vapor. The 40-yr means of intra-annual changes of river levels in 4 watersheds rang from -6.25×10^{-2} m to 1.19×10^{-2} m, consistent with the hypothesis that the long-term average of intra-annual varioans of river leveals is small. This confirms that equation 6 can be used to calculate streamflow according to measurements of precipiation, pan evaporatoion, and river levels.

3.2 Annual and seasonal variations of streamflow

Figure 5 shows measured monthly and annual streamflow averaged over the period from 1961 to 2000 for four watersheds. Overall, streamflow increases from Janary until June and then decreases sharply from July, following the seasonal patterns of precipitation (Fig. 2b). In all watersheds, streamflow peaks in June. The 40-yr means of annual streamflow are 578.35 $m^3 s^{-1}$, 84.08 $m^3 s^{-1}$, 158.71 $m^3 s^{-1}$ and 440.01 $m^3 s^{-1}$ for Meigang, Saitang, Gaosha, and Xiashan watersheds, respectively. The great differences in the magnitudes of streamflow are mainly due to the differences in the scales of four watersheds.

HESSD
8, 9395–9434, 2011

Steamflow shows distinct interannual and decadal variations in all watersheds (Fig. 6). The decadal means of streamflow are higher in 1990s than in other periods for all watersheds (Table 3). Meigang and Saitang watersheds have the lowest streamflow in 1980s (535.65 $m^3 s^{-1}$) and 1970s (72.98 $m^3 s^{-1}$), respectively, while the lowest streamflow appears in 1960s for Gaosha and Xiashan watersheds. Streamflow shows overall increasing trends during the study period of 40 yr in all four watersheds. Streamflow increased at the 5 % signifiance level in Meigang (4.78 $m^3 s^{-1} yr^{-1}$) and Gaosha (1.29 $m^3 s^{-1} yr^{-1}$) watersheds. Streamflow also increased in Saitang and Xiashan watersheds, but less significant.

3.3 Temporal trends of precipitation, pan evaporation and intra-annual changes of river level

Figure 7 shows the temporal trends of annual precipitation, pan evaporation and intra-annual changes of river levels in four watersheds. Annual precipitation increased in all watersheds. In Migang and Gaosha watersheds, annual precipitation increased at the 5 % significance level, with increasing rates equal to 8.05 mm yr^{-1} and 8.65 mm yr^{-1}, respectively. Pan evaporation declined at the 5 % significance level in all watersheds. Saitang watershed had the biggest decline of pan evaporation (−5.86 mm yr^{-1}), followed by Xiashan watershed (−5.31 mm yr^{-1}). Intra-annual changes of river level decreased slowly and insignificantly.

The changing rates of annual total net radiation, actual vapor pressure, mean temperature, and 2 m wind speed during 1961 to 2000 are listed in Table 4. Annual total net radiation and wind speed decreased significantly, with changing rates ranging from $-4.41\,MJ\,m^{-2}\,yr^{-1}$ to $-10.21\,MJ\,m^{-2}\,yr^{-1}$ and from $-8.00\times10^{-3}\,m\,s^{-1}\,yr^{-1}$ to $-1.48\times10^{-2}\,m\,s^{-1}\,yr^{-1}$ among different watersheds, respectively. Actual vapor pressure shows slight and insignificant increasing trends. Annual mean temperature marginally decreased in Saitang watershed (-4.40×10^{-3}° yr^{-1}), while it increased at very small rates in other three watersheds (Table 4).

HESSD
8, 9395–9434, 2011

3.4 Contributions of different climate factors to the changes of streamflow

The contributions of different factors to the changes of streamflow were quantified using Eq. (8) and shown in Table 5. The increase of precipitation and the decreases of evaporation and the intra-annual changes of river level lead to increases in streamflow. Net radiation, actual vapor pressure, temperature and wind speed indirectly impact on streamflow through their roles in evaporation. If evaporation increases with net radiation and wind speed, streamflow will consequently has a reduction trend. As increase/decrease of temperature causes evaporation to increase/decrease, streamflow will correspondingly decreases/increases. However, when evaporation increases/decreases with decrease/increase in actual vapor pressure, streamflow will decrease/increase. In Meigang, Gaosha, and Xiashan watersheds, precipitation has the biggest influence on streamflow, followed by evaporation and then intra-annual change of river level ($P^* > E^* > W^*$,Table 5). The increase of precipitation is the biggest contributor to streamflow increment. This is consistent with previous conclusions by Zhao et al. (2009) that precipitation is the major determinant of streamflow in Poyang Lake Basin. In the Saitang watershed, precipitation increased marginally while actual evaporation decreased significantly, caused by decreasing net radiation and wind speed. The decrease in actual evaporation acts as the biggest contributor to the increase of streamflow ($0.19\,m^3\,s^{-1}\,yr^{-1}$). The inter-annual changes of river level play less important roles in determining streamflow than precipitation and evaporation in all watersheds.

3.5 Variations of streamflow under three different future emission scenarios

Using the Eq. (9), Table 6 lists the changes of projected mean precipitation and evaporation during 2061 to 2100 under three different scenarios of greenhouse gasses emission relative to the mean of precipitation/evaporation observed during 1961 to 2000. The projected future climates by different GCMs exhibit considerable differences. Precipitation and evaporation projected by different GCMs were averaged to generate time

HESSD
8, 9395–9434, 2011

series of integrated precipitation and evaporation. For all four watersheds, precipitation and evaporation were projected to increase under three future climate scenarios. The only exception is the evaporation in Xiashan watershed under the scenario of SRESA2. It was projected to decline. The increases in the precipitation will be the smallest under SRESA2. Similar to precipitation, evaporation will increase to the smallest extent under the scenario of SRESA2. Evaporation will have smaller increases in the Saitang watershed in other three watersheds, and will possibly decrease by 0.28 % in this watershed under the scenario of SRESA2.

Therefore, the future change of streamflow relative to the observed mean during 1961 to 2000 caused by precipitation or evaporation ΔR_i can be calculated with Eq. (10). Figure 8 depicts the calculated ΔR_i values for different climate change scenarios and watersheds. For all the watersheds the projected precipitation changes will cause streamflow to increase under the three future climate scenarios. The largest precipitation-induced increase of streamflow will be under the SRESA1B scenario in the Meigang watershed (+7.16 %) and Xiashan watershed (+6.04 %). The largest precipitation-induced increase of streamflow will be under the SRESB1 scenario in Saitang watershed (+9.13 %) and Gaosha watershed (+6.93 %). However, for three future climate scenarios, evaporation changes will cause streamflow in all watersheds to decrease with the exception of streamflow under the SRESA2 scenario in the Xiashan watershed. In this case, streamflow will increase by 0.16 %. The largest decrease of streamflow caused by evaporation will appear under the scenario of SRESA1B for Meigang (−2.85 %), Saitang (−2.42 %), and Gaosha (−1.89 %) watersheds. Evaporation-induced decrease of streamflow will be the largest under the scenario of SRESB1 in the Xiashan watershed (−2.23 %). The changes of stremflow will be different among watersheds for the same future climate scenario.

With assumption that the future changes of soil water storage can be ignored, the simultaneous changes in averaged-precipitation and evaporation will cause streamflow to increase (Green bars in Fig. 8). Precipitation and evaporation together under the SRESA1B scenario will result in the largest increase in Meigang (+4.31 %) and

HESSD
8, 9395–9434, 2011

Xiashan (+3.84 %) watersheds, while the largest increases of streamflow caused by simultaneous changes of precipitation and evaporation in Saitang (+6.87 %) and Gaosha (+5.15 %) will occur under the SRESB1 scenario.

4 Discussions

Long-term changes in streamflow depend on the balance of precipitation and evaporation. The latter was mainly driven by climatic factors and vegetation characteristics, such as radiation, wind, actual vapor pressure, temperature and vegetation types and density. However, previous researchers mainly focused on the response of streamflow to precipitation, temperature and land cover changes. The influences of other climatic factors (e.g. radiation, wind and actual vapor pressure) on evaporation have received less attention. In this study, we found that the effect of temperature on the streamflow (seen from Table 5) was limited compared with other climate variables (e.g. radiation and wind) in the study area. Because of the complementation between evaporation and runoff from water balance equation, the contribution of temperature to evaporation was also limited. This result is in accordance with the findings of other researchers (Roderick et al., 2002, 2004, 2005a, b, 2007; Sun et al., 2010). The contributions of radiation and wind should be taken into account in investigating the driving factors of streamflow change. On other hand, the observational streamflow trends (dR/dt) can not be exactly explained by the total contributions from precipitation, evaporation and intra-annual river level. This is mainly due to exclusion of the effects of human activities [e.g. agricultural irrigation, water conservancy facilities and land-use change (Guo et al., 2008)], and acclimation of plant physiology (e.g. stomatal) and structures (e.g. LAI) to elevated atmospheric CO_2 concentrations (Gedney et al., 2006; Piao et al., 2007; Field et al., 1995; Cowling et al., 2003) in this study.

Land-use change and establishments of water conservancy facilities can influence the interception of vegetation and the ability of soil infiltration, which played important roles on hydrological regimes, and mechanisms of runoff yield and concentration.

HESSD
8, 9395–9434, 2011

Some studies suggested that land-use changes already impacted the water cycle and will continue to do so in the next century (Costa et al., 1997; Jackson et al., 2005; Foley et al., 2005). Since the late 1960s, Poyang Lake Basin had been used for high head hydropower production and navigation. Until the end of 2005, there were 315 hydropower stations operating in Jiangxi Province, which were above 1000 kW (Zhao et al., 2009). On the other hand, the land-use change would also influence the annual and seasonal flows, although the climate effect was the dominant factor in annual streamflow (Guo et al., 2008). After the Chinese economic reform, the hydropower plants construction, urbanization and population increment etc. would definitely influence the catchments attributes and the water utilization. In order to estimate the contributions of climate changes to streamflow more confidently, we will take account into the roles of vegetation growth feedbacks, land-use change and human activities in streamflow in the future.

5 Conclusions

Based on historical streamflow data of four gauge stations in Poyang Lake Basin, it was shown that streamflow in the four watersheds existed different increasing trends during 1961 to 2000. The streamflow in Meigang and Gaosha watersheds increased at the 5 % significance level, with increasing rates of 4.80 $m^3 s^{-1} yr^{-1}$ and 1.29 $m^3 s^{-1} yr^{-1}$, respectively.

Climate variability induced considerable changes of the terrestrial water cycle in the Poyang Lake Basin. Increasing precipitation is the biggest contributor to streamflow increment in Meigang Gaosha, and Xiashan watershed, while decreasing evaporation is the main reason of streamflow increment in Saitang watershed. The changes caused by intra-annual changes of river levels were the smallest and evenly can be negligible. Radiation and wind reduction caused streamflow to increase. However, evaporation decrease/increase caused by the increase/decrease of actual vapor pressure and mean temperature lead streamflow to an increase/decrease. Radiation and

HESSD
8, 9395–9434, 2011

wind have larger contributions than actual vapor pressure and mean temperature in affecting evaporation and stremflow.

The projected climates by different GCMs under three future climate scenarios, including medium greenhouse gases emission scenario (SRESA1B), high greenhouse gases emission scenario (SRESA2), and low greenhouse gases emission scenario (SRESB1) were used to assess the future changes of streamflow in the study area. Without the consideration of the changes of soil water storage in future, with the increasing precipitation and the increasing evaporation (not including the SRESB1 in Xiashan watershed), the streamflow shows an uptrend. Furthermore, the largest increases in streamflow of Meigang watershed (+4.13 %) and Xiashan watershed (+3.84 %) appear under SRESA1B scenario. The increase in streamflow Saitang watershed (+6.87 %) and Gaosha watershed (+5.15 %) will occur under the SRESB1 scenario.

Acknowledgements. This paper is financially supported by National Natural Science Foundation of China, (Grant No. 40775061/D0507 & Grant No. 41075082). Some of calculations are performed in Key Laboratory of Meteorological Disaster of Ministry of Education, Nanjing University of Information Science & Technology. The authors would like to thank all the data providing agencies and bodies.

References

Allen, R. G., Pereira, L. S., Raes, D., and Smith, M.: Crop evapotranspiration-guidelines for computing crop water requirements-FAO Irrigation and Drainage Paper 56. FAO, 1998, ISBN 92-5-104219-5, 1998.

Andréasson, J., Bergström, S. B., Carlsson, B., Graham, L. P., and Lindström, G.: Hydrological change-climate change impact simulations for Sweden, Ambio, 33, 228–234, 2004.

Arnell, N. W.: Climate change and global water resources, Global Environ. Chang., 9 (Supplement 1), 531–549, 1999.

Chen, H., Guo, S., Xu, C., and Singh, V. P.: Historical temporal trends of hydro-climatic variables

HESSD

8, 9395–9434, 2011

and runoff response to climate variability and their relevance in water resource management in the Hanjiang Basin, J. Hydrol., 344, 171–184, 2007.
Christensen, N. S. and Lettenmaier, D. P.: A multimodel ensemble approach to assessment of climate change impacts on the hydrology and water resources of the Colorado River Basin, Hydrol. Earth Syst. Sci., 11, 1417–1434, doi:10.5194/hess-11-1417-2007, 2007.
Costa, M. H. and Foley, J. A.: Water balance of the Amazon Basin: Dependence on vegetation cover and canopy conductance, J. Geophys. Res., 102, 23973–23989, 1997.
Crockford, R. H. and Richardson, D. P.: Partitioning of rainfall into throughfall, streamflow and interception: effect of forest type, ground cover and climate, Hydrol. Process., 14, 2903–2920, 2000.
Cowling, S. A. and Field, C. B.: Environmental control of leaf area production: Implications for vegetation and land-surface modeling, Global Biogeochem. Cy., 17, 1007, doi:10.1029/2002GB001915, 2003.
Ding, Y. and Dai, X.: Temperature variation in China during the last 100 years, Meteorological Monthly, 20, 19–26, 1994 (in Chinese).
Fan, S., Gao, Y., Cheng, Y., and Bai, Q.: Rainfall-intercepting capability of forest canopy, Scientia Geographica Sinica, 27, 200–204, 2007 (in Chinese).
Field, C. B., Jackson, R. B., and Mooney, H. A.: Stomatal responses to increased CO_2: implications from the plant to the global scale, Plant. Cell Environ., 18, 1214–1225, 1995.
Foley, J. A., DeFries, R., Asner, G. P., Barford, C., Bonan, G., Carpenter, S. R., Chapin, F. S., Coe, M. T., Daily, G. C., Gibbs, H. K., Helkowski, J. H., Holloway, T., Howard, E. A., Kucharik, C. J., Monfreda, C., Patz, J. A., Prentice, I. C., Ramankutty, N., and Snyder, P. K.: Global consequences of land use, Science, 309, 570–574, 2005.
Frederick, K. D. and Major, D. C.: Climate change and water resources, Climate Change, 37, 7–23, 1997.
Gao, X., Zhao, Z., Ding, Y., Huang, R., and Filippo, G.: Climate change due to greenhouse effects in China as simulated by a regional climate model, Advance in Atmosphere Sciences, 18, 1224–1230, 2001.
Gedney, N., Cox, P. M., Betts, R. A., Huntingford, C., and Stott, P. A.: Detection of a direct carbon dioxide effect in continental river runoff records, Nature, 439, 835–838, 2006.
Gül, G. O., Rosbjerg, D., Gül, A., Ondracek, M., and Dikgola, K.: Assessing climate change impacts on river flows and environmental flow requirements at catchment scale, Ecohydrology, 3, 28–40, 2010.

HESSD
8, 9395–9434, 2011

Guo, H., Qi, H., and Jiang, T.: Annual and seasonal streamflow responses to climate and land-cover changes in the Poyang Lake basin, China, J. Hydrol., 355, 106–122, 2008.
Guo, S., Chen, H., Zhang, H., Xiong, L., Liu, P., Pang, B., Wang, G., and Wang, Y.: A semi-distributed monthly water balance model and its application in a climate change impact study in the middle and lower Yellow River basin, Water Int., 30, 250–260, 2005.
Hölscher, D., Köhler, L., van Dijk, A. I. J. M., and Bruijnzeel, L. A.: The importance of epiphytes to total rainfall interception by a tropical montane rain forest in Costa Rica, J. Hydrol., 292, 308–332, 2004.
Hu, Q., Feng, S., Guo, H., Chen, G., and Jiang, T.: Interactions of the Yangtze river flow and hydrologic processes of the Poyang Lake, China, J. Hydrol., 347, 90–100, 2007.
Huang, Y. S., Chen, S. S., and Lin, T. P.: Continuous monitoring of water loading of trees and canopy rainfall interception using the strain gauge method, J. Hydrol., 311, 1–7, 2005.
IPCC.: Climate Change 2001: The Scientific Basis. Summary for Policymakers and Technical Summary of Working Group I Report. Cambridge, UK: Cambridge University Press, 2001.
Jackson, R. B., Jobbágy, E. G., Avissar, R., Roy, S. B., Barrett, D., Cook, C. W., Farley, K. A., Maitre, D. C. L., McCarl, B. A., and Murray, B. C.: Trading water for carbon with biological carbon sequestration, Science, 310, 1944–1947, 2005.
Jiang, T. and Shi, Y.: Global warming and its consequences in Yangtze River floods and damages, Advance in Earth Sciences, 18, 277–284, 2003 (in Chinese).
Jiang, Z.: Analysis and research about loading ability of the water environment of Poyang Lake. Nanchang University, Nanchang, China, 13 pp., 2007 (in Chinese with English abstract).
Kundzewicz, Z. W., Mata, L. J., Arnell, N. W., Döll, P., Kabat, P., Jiménez, B., Miller, K. A., Oki, T., Sen, Z., and Shiklomanov, I. A.: Freshwater resources and their management, in: Climate Change 2007: Impacts, Adaptation and Vulnerability. Contribution of Working Group II to the Fourth Assessment Report of the Intergovernmental Panel on Climate Change, edited by: Parry M. L., Canziani, O. F., Palutikof, J. P., van der Linden, P. J., and Hanson, C. E., Cambridge University Press, Cambridge, UK, 73–210, 2007.
Li, J., Liu, Y., Yang, X., and Li, J.: Studies on water vapor flux characteristic and the relationship with environment factors over a planted coniferous forest in Qianyanzhou station, Acta Ecologica Sinica, 26, 2449–2456, 2006 (in Chinese).
Li. Q., Li, W., Si, P., Gao, X., Dong, W., Jones, P., Huang, J., and Cao, L.: Assessment of surface air warming in northeast China, with emphasis on the impacts of urbanization, Theor. Appl. Climatol., 99, 469–478, 2010.

HESSD
8, 9395–9434, 2011

Lins, H. F. and Slack, J. R.: Streamflow trends in the United States, Geophys. Res. Lett., 26, 227–230, 1999.
Liu, C. and Fu, G.: Analysises of hydrological response to climatic changes in China, in: Climate change and influence, edited by: Zhang, Y. and Zhang, P., China Meteorological Press, Beijing, China, 205–213, 1993 (in Chinese).
Liu, Q. and Cui. B.: Impacts of climate change/variability on the streamflow in the Yellow River Basin, China, Ecol. Modell., 222, 268–274, 2009.
Milly, P. C. D., Dunne, K. A., and Vecchia, A. V.: Global pattern of trends in streamflow and water availability in a changing climate, Nature, 438, 347–350, 2005.
Nash, L. L. and Gleick, P. H.: Sensitivity of streamflow in the Colorado Basin to climate change, J. Hydrol., 125, 221–241, 1991.
Null, S. E, Viers J. H., and Mount, J. F.: Hydrologic response and watershed sensitivity to climate warming in California's Sierra Nevada, PLoS ONE, 5, 1–16, 2010.
Oki, T. and Kanae, S.: Global hydrological cycles and world water resources, Science, 313, 1068–1071, 2006.
Oki, T., Musiake K., Matsuyama, H., and Masuda, K.: Global atmospheric water balance and runoff from large river basins, Hydrol. Process., 9, 655–678, 1995.
Piao, S., Friedlingstein, P., Ciais, P., de Noblet-Ducoudré, N., Labat, D., and Zaehle, S.: Changes in climate and land use have a larger direct impact than rising CO_2 on global river runoff trends, Proc. Natl. Acad. Sci., 104, 15242–15247, 2007.
Roderick, M. L. and Farquhar, G. D.: The cause of decreased pan evaporation over the past 50 years, Science, 298, 1410–1411, 2002.
Roderick, M. L. and Farquhar, G. D.: Changes in Australian pan evaporation from 1970 to 2002, Int. J. Climatol., 24, 1077–1090, 2004.
Roderick, M. L. and Farquhar, G. D.: Changes in New Zealand pan evaporation since the 1970s, Int. J. Climatol., 25, 2031–2039, 2005.
Roderick, M. L., Farquhar, G. D., and Hobbins, M. T.: On the attribution of changing pan evaporation, Geophys. Res. Lett., 34, L17403, doi:10.1029/2007GL031166, 2007.
Rui, X.: Hydrology Principle. China Waterpower press, Beijing, China, 14–17, 2005 (in Chinese).
Shankman, D., Keim, B. D., and Song, J.: Flood frequency in China's Poyang Lake Region: trends and teleconnections, Int. J. Climatol., 26, 1255–1266, 2006.
Sun, S. L., Zhou, S. Q., Song, J., Shi, J. H., Gu, R. Y., and Ma, F. M.: Change in pan evaporation

HESSD
8, 9395–9434, 2011

and its driving factors in Jiangxi Province, Transactions of the Chinese Society of Agricultural Engineering, 26, 59–65, 2010 (in Chinese).
The Standing Committee of the National People's Congress (NPC) of the People's Republic of China.: The 21st Agenda of China – Population, Environment and Development White Paper. Beijing, China, 1994 (in Chinese).
Thodsen, H.: The influence of climate change on stream flow in Danish rivers, J. Hydrol., 333, 226–238, 2007.
Vörösmarty, C. J., Green, P., Salisbury, J., and Lammers, R. B.: Global water resources: vulnerability from climate change and population growth, Science, 289, 284–288, 2000.
Wang, S. and Dong, D.: Enhancement of the warming trend in China, Geophys. Res. Lett., 27, 2581–2584, 2000.
Wen, Y. and Liu, S.: Quantitative analysis of the characteristics of rainfall interception of main forest ecosystems in China, Scientia Silvae Sinicae, 31, 289–298, 1995 (in Chinese).
Xiong, L. and Guo S.: Two-parameter water balance model and its application, J. Hydrol., 216, 111–123, 1999.
Xiong, L. and Guo, S.: Trend test and change-point detection for the annual discharge series of the Yangtze River at the Yichang hydrological station, Hydrolog. Sci. J., 49, 99–112, 2004.
Xu, C., Gong, L., Jiang, T., Chen, D., and Singh, V. P.: Analysis of spatial distribution and temporal trend of reference evapotranspiration and pan evaporation in Changjiang (Yangtze River) catchment, J. Hydrol., 327, 81–93, 2006.
Xu, Z., Liu, Z., Fu, G., and Chen, Y.: Trends of major hydroclimatic variables in the Tarim River Basin during the past 50 years, Journal of Arid Environments, 74, 256–267, 2010.
Yang, X., Zhang, Y., Ding, M., Liu, L., Wang, Z., and Gao, D.: Observation evidence of the impact of vegetation cover on surface air temperature change in China, Chinese J. Geogr.-CH, 53, 833–841, 2010 (in Chinese).
Zhai, P., Chao, Q., and Zou, X.: Progress in China's climate change study in the 20th century, J. Geogr. Sci., 14, 3–11, 2004.
Zhao, G., Hörmann, G., Fohrer, N., and Zhai, J.: Streamflow trends and climate variability impacts in Poyang Lake Basin, China, Water Resour. Manage., 24, 689–706, 2009.
Zhang, J., Dong, W., Wu, L., Wei, J., Chen, P., Lee, and D. K.: Impact of land use changes on surface warming in China, Adv. Atmos. Sci., 22, 343–348, 2005.
Zhang, W., Xiao, Z., Zheng, J., and Ren, J.: Long-term variation features of streamflow and its response to climate change in Nujiang Basin, Science Bullet., 52 (Supplement II), 135–141,

HESSD
8, 9395–9434, 2011

2007 (in Chinese with English Abstract).
Zhang, X., Harvey, K. D., Hogg, W. D., and Yuzyk, T. R.: Trends in Canadian streamflow, Water Resour. Res., 37, 987–998, 2001.

HESSD
8, 9395–9434, 2011

Table 1. General circulation models and their projected climates used in this study.

Models	20C3M (1961 ~ 2000)	3 future climate scenarios (2061 ~ 2100)		
		SRESA1B	SRESA2	SRESB1
cccma_cgcm3.1_t63	*	*		*
mpi_echam5	*	*	*	*
miub_echo_g	*	*		*
miroc3_2_medres	*	*	*	*
miroc3_2_hires	*	*		*
ipsl_cm4	*	*	*	*
inmcm3_0	*	*	*	*
ingv_echam4	*	*	*	
giss_model_e_r	*	*	*	*
giss_aom	*	*		*
gfdl_cm2_0	*	*	*	*

Note: * denotes that the climate projected by a model was used in this study.

HESSD
8, 9395–9434, 2011

Table 2. The parameters in Eq. (6) optimized for four watersheds in the study area.

	Parameters	Meigang	Saitang	Gaosha	Xiashan
1961 ~ 1990	*a*	0.96**	0.82**	0.82**	0.85**
	b	0.38**	0.30**	0.33**	0.34**
	c	−0.15**	−0.32**	−0.19*	−0.11**
1961 ~ 2000	*a*	0.98**	0.84**	0.79**	0.82**
	b	0.40**	0.32**	0.29**	0.32**
	c	−0.14**	−0.30**	−0.22**	−0.12**

Note: * and ** denote signifiance levels of 5 % and 1 %, respectively.

HESSD
8, 9395–9434, 2011

Table 3. Decadal variations of streamflow in four watersheds.

	1961 ~ 1970 ($m^3 s^{-1}$)	1971 ~ 1980 ($m^3 s^{-1}$)	1981 ~ 1990 ($m^3 s^{-1}$)	1991 ~ 2000 ($m^3 s^{-1}$)	1961 ~ 2000 ($m^3 s^{-1}$)
Meigang	538.72	549.05	535.65	689.97	578.35
Saitang	83.32	72.98	84.54	95.48	84.08
Gaosha	146.06	151.38	148.49	188.93	158.71
Xiashan	404.58	443.46	439.97	472.04	440.01

HESSD
8, 9395–9434, 2011

Table 4. Changes of annual total net radiation, mean actual vapor pressure, mean temperature, and mean 2 m wind speed with time during 1961 to 2000.

	climate variability			
	dR_n/dt (MJ m^{-2} yr^{-1})	de_a/dt (kPa yr^{-1})	dT_{ave}/dt ($^\circ$ yr^{-1})	dU/dt (m s^{-1} yr^{-1})
Meigang	-9.03^{**}	-5.00×10^{-3}	3.90×10^{-3}	$-9.60\times10^{-3**}$
Saitang	-10.21^{**}	-1.00×10^{-4}	-4.40×10^{-3}	$-1.43\times10^{-2**}$
Gaosha	-4.41^{*}	-6.00×10^{-5}	2.60×10^{-3}	$-8.00\times10^{-3**}$
Xiashan	-9.26^{**}	-8.00×10^{-4}	1.70×10^{-3}	$-1.48\times10^{-2**}$

Note: * and ** represent the signifiance levels of 5 % and 1 %, respectively.

HESSD
8, 9395–9434, 2011

Table 5. The variations of streamflow caused by the changes of precipitation, evaporation and inter-annual river levels (Units: $m^3\ s^{-1}\ yr^{-1}$).

	P^*	E^*	Effects of climatic factors on streamflow through evaporation processes				W^*
			R_n^*	e_a^*	T_{ave}^*	U^*	
Meigang	3.79	0.82	0.59	−0.12	−0.20	0.51	0.68
Saitang	0.13	0.19	0.09	−0.004	0.05	0.06	0.10
Gaosha	1.12	0.21	0.05	−0.003	−0.01	0.10	0.12
Xiashan	1.34	0.86	0.66	−0.16	−0.06	0.68	0.22

HESSD
8, 9395–9434, 2011

Table 6. Percent changes of precipitation and evaporation projected under different greenhouse gasses emission scenarios.

	Watershed		SRESA1B	SRESA2	SRESB1
Precipitation	Meigang/%	Range	−2.07 ~ 12.46	−2.86 ~ 10.79	−0.50 ~ 12.43
		Average	4.78	2.30	4.42
	Saitang/%	Range	− 5.69~ 9.42	− 4.60~ 11.69	− 0.31~ 17.90
		Average	3.83	2.44	6.00
	Gaosha/%	Range	−5.36 ~ 12.66	−3.1 ~ 8.44	−1.56 ~ 14.39
		Average	4.95	2.67	5.04
	Xiashan/%	Range	−5.36 ~ 11.47	−6.85 ~ 10.20	−3.32 ~ 12.01
		Average	3.88	1.36	3.11
Evaporation	Meigang/%	Range	−0.03 ~ 11.61	−2.44 ~ 10.11	−1.39 ~ 8.58
		Average	5.8	1.81	5.27
	Saitang/%	Range	−0.37 ~ 14.52	−7.56 ~ 12.85	−1.11 ~ 11.24
		Average	4.67	1.30	4.36
	Gaosha/%	Range	0.26 ~ 12.34	−7.99 ~ 11.50	−1.52 ~ 9.62
		Average	5.02	1.91	4.75
	Xiashan/%	Range	−0.76 ~ 11.55	−7.58 ~ 7.48	−0.73 ~ 8.68
		Average	3.91	−0.28	3.96

HESSD
8, 9395–9434, 2011

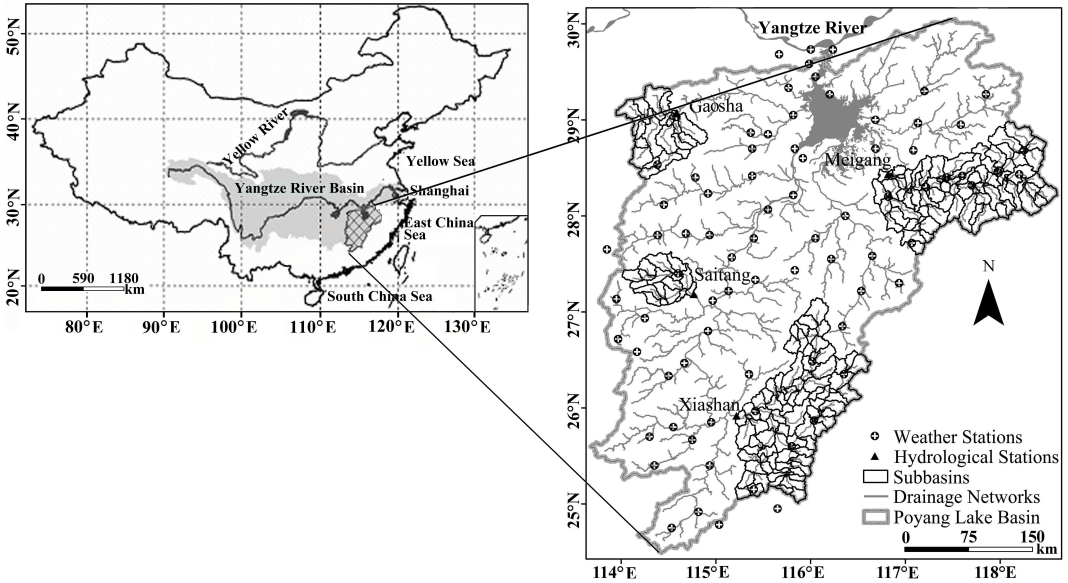

Fig. 1. The study area, Poyang Lake Basin located in southern China. 79 weather stations and 4 gauge stations are also shown.

HESSD
8, 9395–9434, 2011

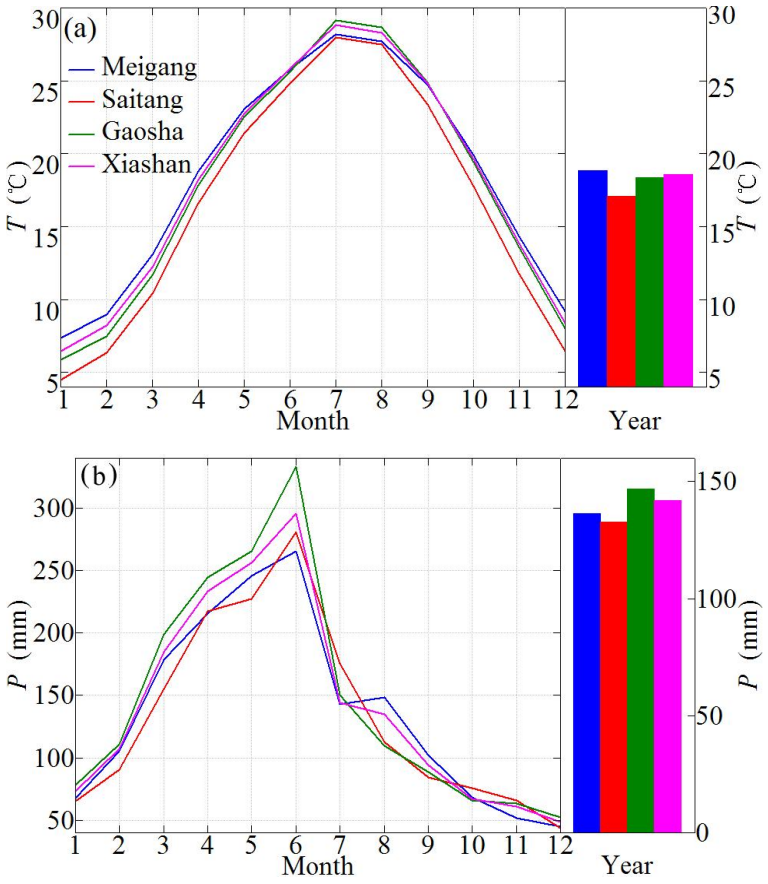

Fig. 2. Monthly and annual mean temperatures **(a)** and precipitation **(b)** averaged during the period from 1961 to 2000 for four typical watersheds in the study area.

HESSD
8, 9395–9434, 2011

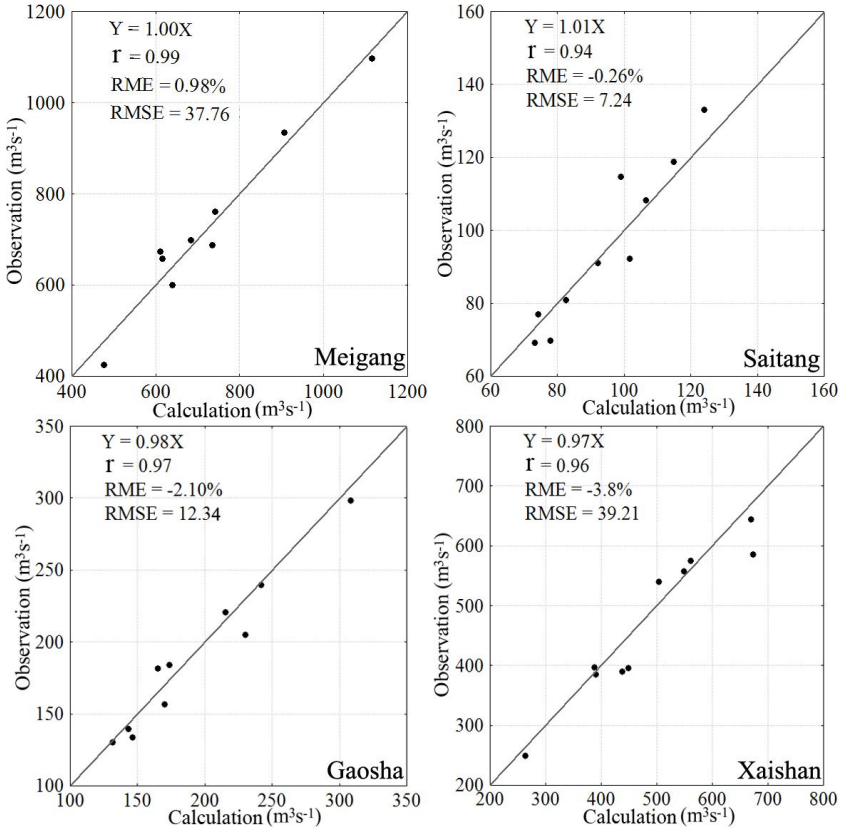

Fig. 3. Comparison of observed and calculated annual mean streamflow during the period from 1991 to 2000. The solid lines are the 1:1 lines. RME and RMSE were calculated as $\mathrm{RME} = \frac{1}{n}\left(\sum_{i=1}^{n}\frac{R_{\mathrm{OBS},i}-R_{\mathrm{CAL},i}}{R_{\mathrm{OBS},i}}\right)$ and $\mathrm{RMSE} = \sqrt{\frac{1}{n}\sum_{i=1}^{n}\left(R_{\mathrm{OBS},i}-R_{\mathrm{CAL},i}\right)^2}$ respectively. $R_{\mathrm{OBS},i}$ and $R_{\mathrm{CAL},i}$ are the observed and calculated streamflow values, $n = 10$.

HESSD
8, 9395–9434, 2011

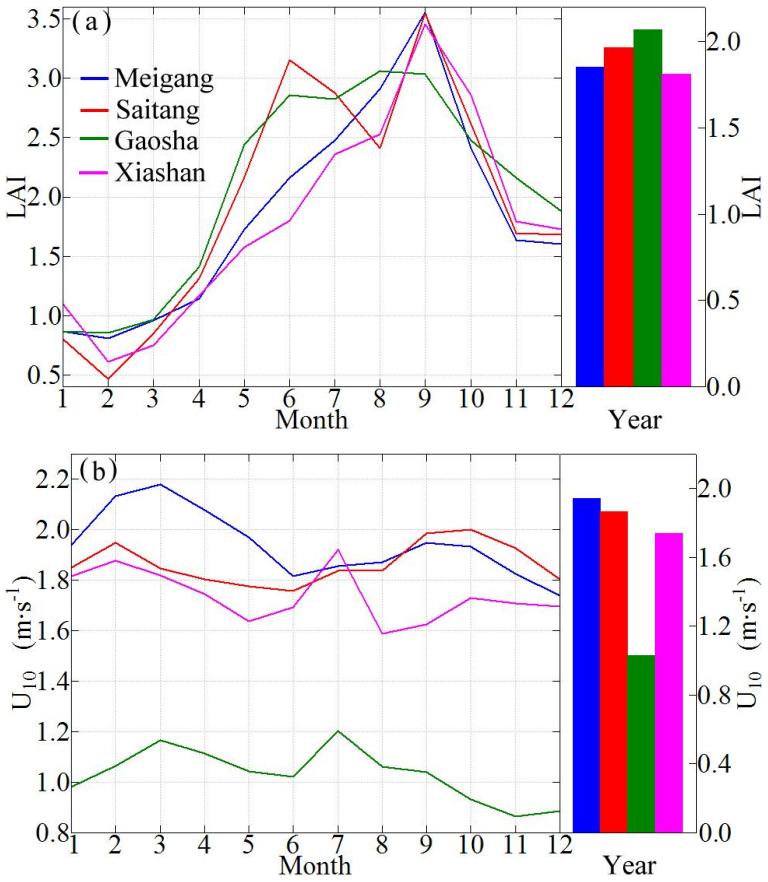

Fig. 4. Seasonal variations and annual means of LAI (1999 ~ 2000) **(a)** and 10 m wind speed (1961 ~ 2000) **(b)** in four watersheds.

HESSD
8, 9395–9434, 2011

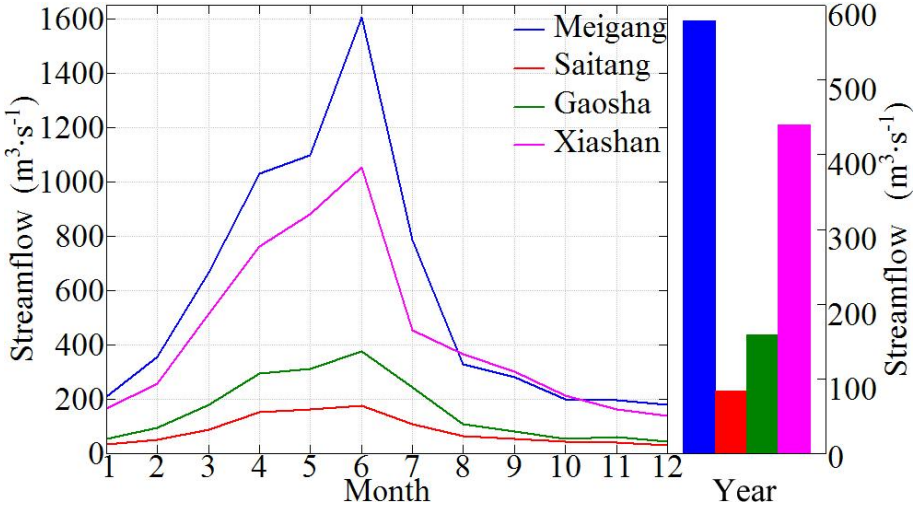

Fig. 5. Monthly and annual streamflow averaged over the period from 1961 to 2000.

HESSD
8, 9395–9434, 2011

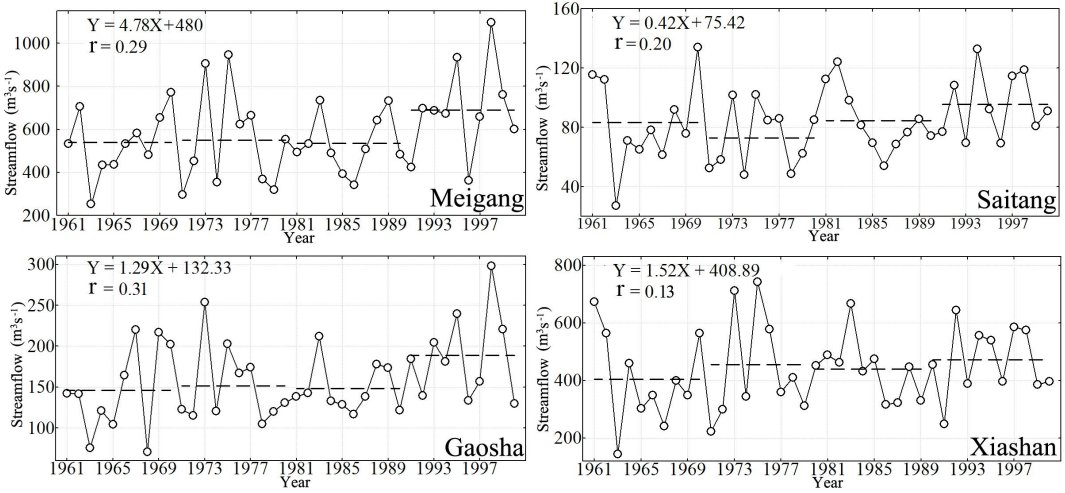

Fig. 6. Annual mean streamflow during the period from 1961 to 2000.

HESSD
8, 9395–9434, 2011

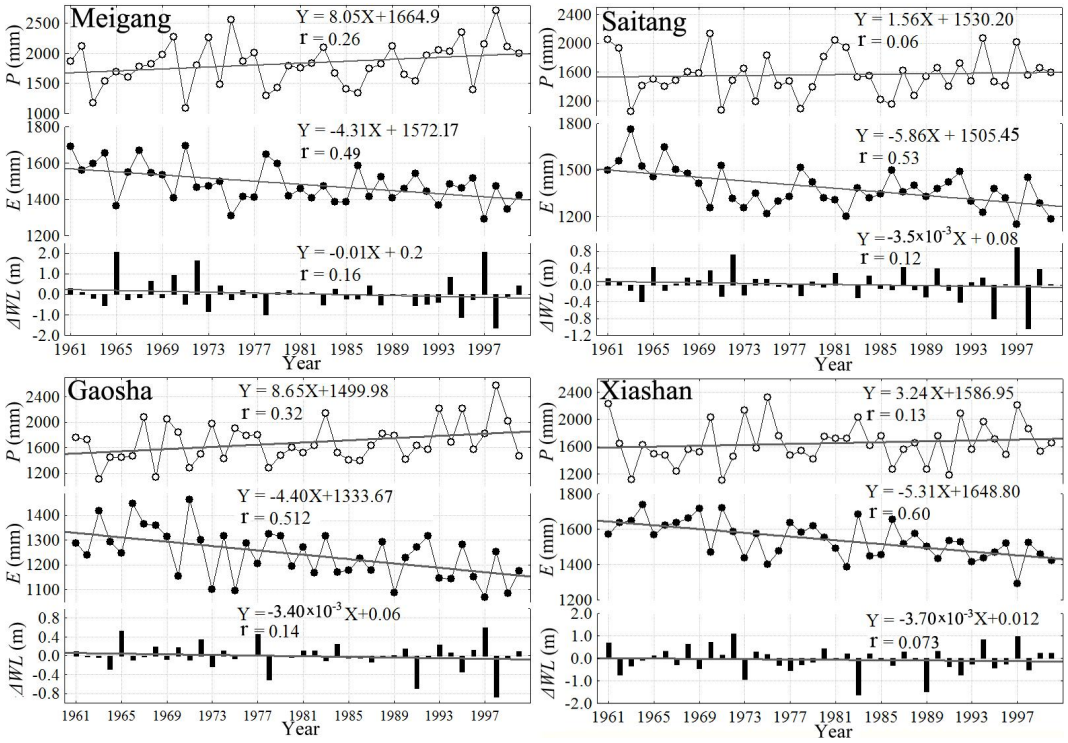

Fig. 7. Annual means of precipitation, pan evaporation and intra-annual changes of river level during 1961 to 2000.

HESSD
8, 9395–9434, 2011

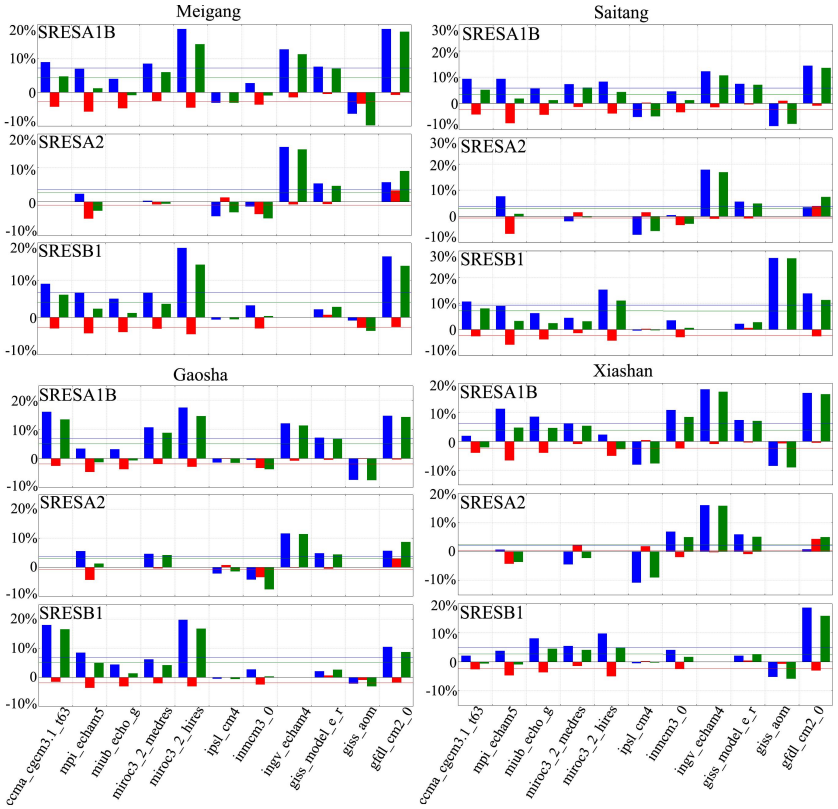

Fig. 8. Changes of streamflow in four watersheds caused by changes of precipitation and evaporation projected under different greenhouse gasses emission scenarios. Blue, red, and green bars represent changes of streamflow caused by changes of precipitation, evaporation, and both precipitation and evaporation projected by individual GCMs, respectively. Blue, red, and green lines represent the averaged changes of streamflow caused by changes of precipitation, evaporation, and both precipitation and evaporation, respectively.

HESSD
8, 9395–9434, 2011